ACS Infectious Diseases

Open Access
This article is licensed under CC-BY-NC-ND 4.0

pubs.acs.org/journal/aidcbc
Article

# *In Vivo* Bioluminescence Imaging Reveals Differences in *Leishmania infantum* Parasite Killing Kinetics by Antileishmanial Reference Drugs

*Published as part of ACS Infectious Diseases virtual special issue "One Health and Vector Borne Parasitic Diseases".*

Sarah Hendrickx, Pim-Bart Feijens, Fanny Escudié, Eric Chatelain, Louis Maes, and Guy Caljon*

Cite This: *ACS Infect. Dis.* 2024, 10, 2101−2107

Read Online

ACCESS | Metrics & More | Article Recommendations | Supporting Information

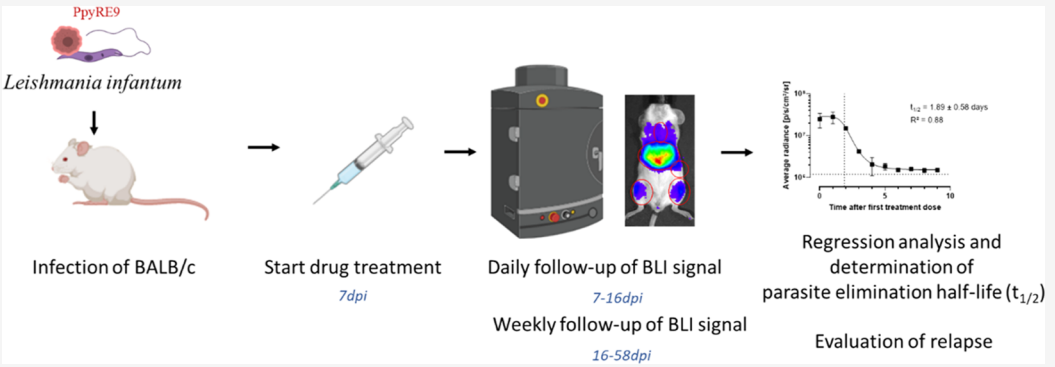


**ABSTRACT:** The bioluminescent *Leishmania infantum* BALB/c mouse model was used to evaluate the parasiticidal drug action kinetics of the reference drugs miltefosine, paromomycin, sodium stibogluconate, and liposomal amphotericin B. Infected mice were treated for 5 days starting from 7 days post-infection, and parasite burdens were monitored over time *via* bioluminescence imaging (BLI). Using nonlinear regression analyses of the BLI signal, the parasite elimination half-life ($t_{1/2}$) in the liver, bone marrow, and whole body was determined and compared for the different treatment regimens. Significant differences in parasiticidal kinetics were recorded. A single intravenous dose of 0.5 mg/kg liposomal amphotericin B was the fastest acting with a $t_{1/2}$ of less than 1 day. Intraperitoneal injection of paromomycin at 320 mg/kg for 5 days proved to be the slowest with a $t_{1/2}$ of about 5 days in the liver and 16 days in the bone marrow. To conclude, evaluation of the cidal kinetics of the different antileishmanial reference drugs revealed striking differences in their parasite elimination half-lives. This BLI approach also enables an in-depth pharmacodynamic comparison between novel drug leads and may constitute an essential tool for the design of potential drug combinations.

**KEYWORDS:** *Leishmania, BLI, bioluminescence, TTK, pharmacodynamics*

With several new chemical entities (NCE) (co)developed by the Drugs for Neglected Diseases initiative (DNDi) entering clinical development against visceral leishmaniasis (VL),[1] focus is now shifting toward in-depth characterization of advanced leads and clinical candidates. Previous studies, including those of our group, already compared the pharmacodynamics and *in vitro* time-to-kill (TTK) of DNDi drug leads with routinely used antileishmanial reference drugs and identified their putative modes of action.[2−5] Although *in vitro* TTK studies may offer some insights for the design of combination therapies, the present study explored the bioluminescent VL BALB/c mouse model to evaluate the parasiticidal dynamics of the most commonly used antileishmanial reference drugs. Since the introduction of reporter gene technology, our group has shown that *in vivo* bioluminescent imaging (BLI) of VL-infected laboratory animals enables noninvasive longitudinal follow-up of drug activity in various target organs with identification of sanctuary sites and monitoring of post-treatment relapse.[6,7] For all target organs, a significant positive correlation was found between microscopy, SL-RNA qPCR, and BLI, indicating that BLI can be used to evaluate not only parasite multiplication but also

**Received:** February 7, 2024
**Revised:** May 2, 2024
**Accepted:** May 3, 2024
**Published:** May 11, 2024

ACS Publications
© 2024 American Chemical Society



https://doi.org/10.1021/acsinfecdis.4c00109
*ACS Infect. Dis.* 2024, 10, 2101−2107

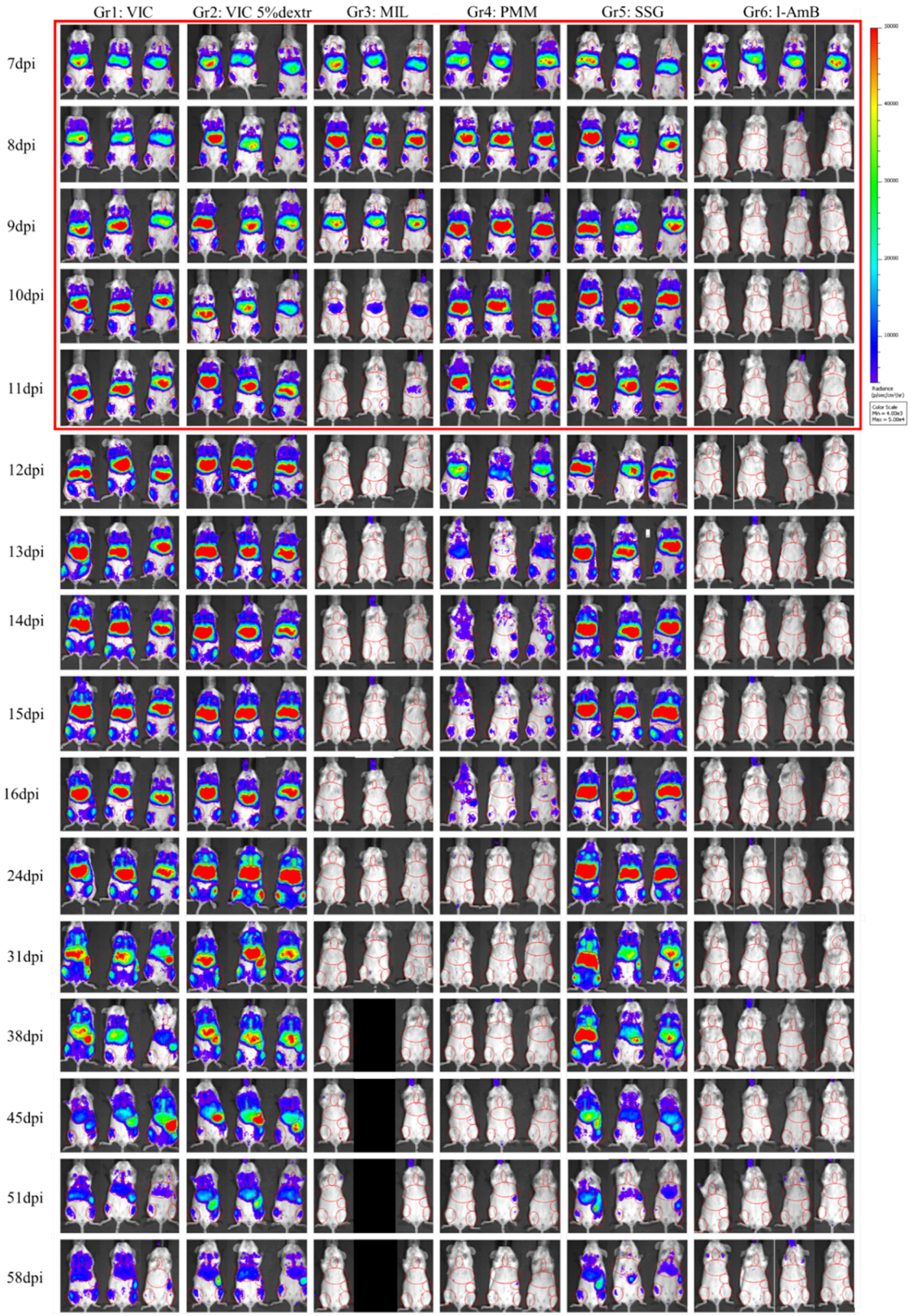


**Figure 1.** Bioluminescent signal measured of individual mice in all treatment groups throughout the course of the experiment. The treatment period is indicated by the red square. The red circles in individual images indicate the measured regions of interest (ROI) in individual animals. At 38 dpi, one mouse from the miltefosine group died during anesthesia for reasons unrelated to infection. BLI scale: $4e^3$-$5e^4$ relative light units (RLU; $p/s/cm^2/sr$) (Gr: group; VIC: vehicle-administered control; MIL: miltefosine; PMM: paromomycin; SSG: sodium stibogluconate; l-AmB: liposomal amphotericin B; dpi: days post-infection).



https://doi.org/10.1021/acsinfecdis.4c00109
ACS Infect. Dis. 2024, 10, 2101−2107

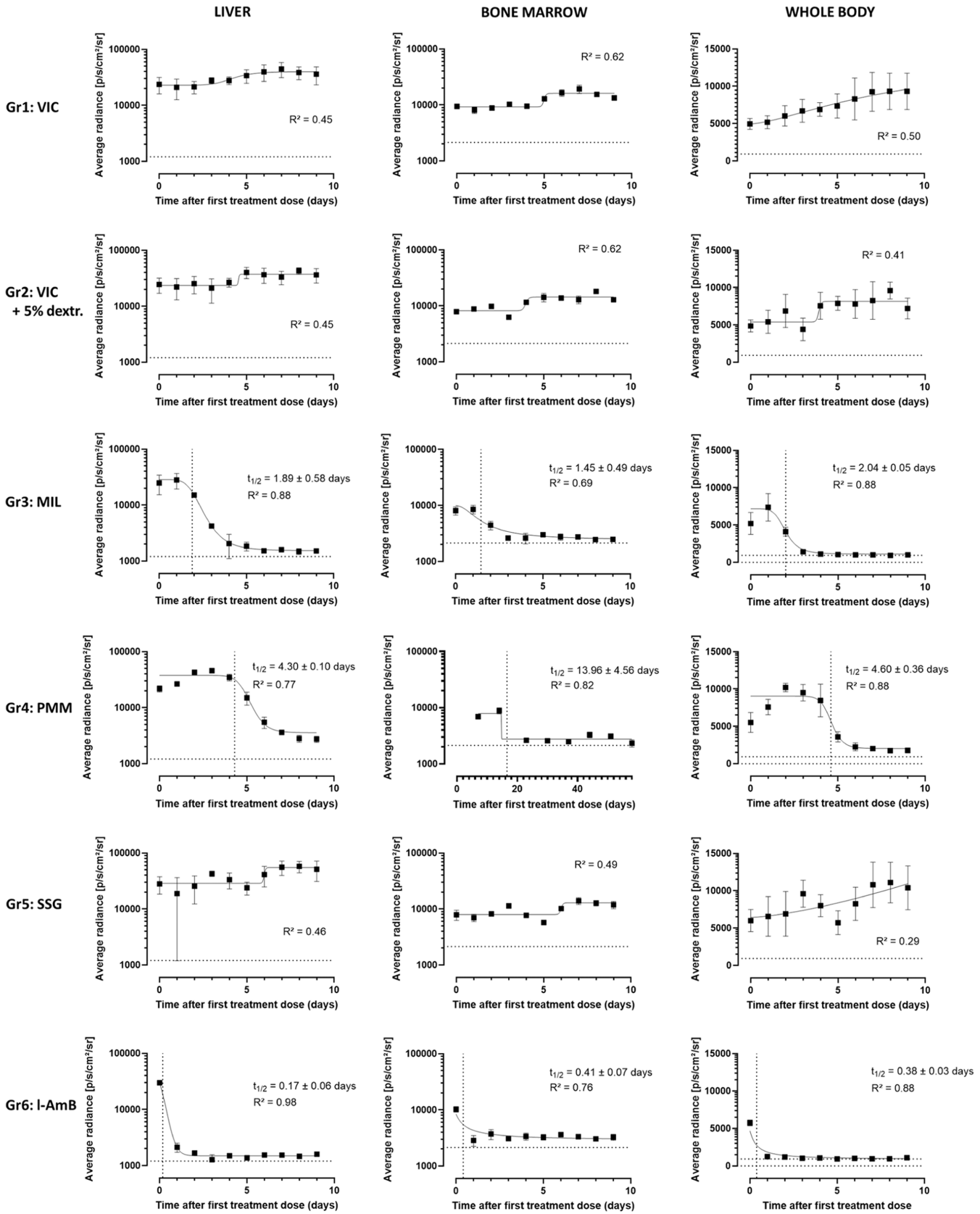


**Figure 2.** Average bioluminescent signal measured in the liver, the bone marrow, and the whole body for both vehicle groups and upon treatment with miltefosine (MIL), paromomycin (PMM), sodium stibogluconate (SSG), and liposomal Amphotericin B (l-AmB). The kinetics of parasite killing were evaluated and compared between the drugs based on nonlinear regression analysis. A parasite elimination half-life ($t_{1/2}$) was estimated for each drug treatment in each specific region of interest (ROI). The dotted line represents the radiance detected in noninfected control animals over the course of the experiment.



https://doi.org/10.1021/acsinfecdis.4c00109
ACS Infect. Dis. 2024, 10, 2101−2107

parasite survival upon drug treatment.[7] This *in vivo* study used the bioluminescent *Leishmania infantum* BALB/c mouse model to evaluate the cidal kinetics of the antileishmanial reference compounds sodium stibogluconate (SSG), miltefosine (MIL), paromomycin (PMM) and liposomal amphotericin B (l-AmB) using an SGG-resistant *Leishmania* clinical isolate. As resistance toward antimonials is very common in some areas, it is pivotal to demonstrate activity against SSG-resistant strains. The ultimate goal of this study was to establish a model to characterize the antileishmanial properties of novel chemotherapeutic lead candidates. Our results show that the *in vivo* BLI mouse model has the potential to discriminate different drugs based on their parasite clearance rate in the liver, bone marrow, and whole body and can also be used to predict post-treatment relapse, making it a supportive tool in the search of novel drugs against VL.

## RESULTS AND DISCUSSION

Figure 1 shows the average bioluminescence levels recorded over time for both vehicle control groups (Gr1, Gr2) and the groups treated with MIL (Gr3), PMM (Gr4), SGG (Gr5), and l-AmB (Gr6). The signals in both control groups indicate a reproducible infection in the target organs and a progressive increase, indicative of rising parasite burdens. The assay window is characterized by a high BLI signal in regions of interest (ROI) corresponding to the liver, bone marrow, and whole body in the absence of drug treatment. The established assay window therefore enables characterizing drug activity without the impact of self-resolution that is characteristic of a later phase of a BALB/c VL infection. All treatment groups show a decline in BLI signal over time, except the SSG group that remained comparable to the vehicle-treated infected groups linked to the use of an SSG-resistant strain (Figures 1 and 2). BLI follow-up of MIL-treated mice indicates a rapid cidal activity in all ROIs with a reduction of the signal to the level of noninfected control mice within the 5 day treatment period and parasite elimination half-life ($t_{1/2}$) values of 2.0 days in the whole body, 2.0 days in the liver, and 1.2 days in the bone marrow (Table 1 and Figure 2) with a relatively quick decrease in BLI signal down to levels measured in uninfected control animals (Figure 3). Unfortunately, one mouse died under anesthesia during follow-up. Looking at a more sensitive scale on 58 dpi (Figure 3), no parasite-specific BLI signal can be detected. However, one mouse did harbor detectable residual amastigotes in the liver, suggesting that post-treatment relapse could still be possible when extending the time of follow-up. PMM treatment on the contrary resulted in a delayed systemic parasite clearance with the decline of BLI signal only starting after the last day of treatment and baseline BLI levels being reached only by 23 days post-infection (dpi). A $t_{1/2}$ of 4.6 days could be identified at whole body level while 4.8 days in the liver and 16.6 days in the bone marrow (Table 1 and Figure 2). Together with the detectable parasites in the bone marrow at the more sensitive BLI scale (Figure 3) at 58 dpi and in Giemsa-stained spleen and bone marrow samples (with on average 0.01 ± 0.008 amastigotes/cell in the spleen and 0.007 amastigotes/cell in the bone marrow), this indicates that PMM is much less effective at the used dose. These results corroborate earlier work performed *in vitro*, where the cidal activity of MIL on intracellular amastigotes was faster than that of PMM.[4] This observation is in line with our previous research showing the presence of quiescent parasites in the bone marrow and identifying the bone marrow as a source for PMM post-treatment relapse.[5] The intrinsically high limit of detection (LoD) of the technique (LoD of ~$10^7$ amastigotes in the liver and ~$10^4$ parasites in the spleen)[7] implies that the absence of a BLI signal does not necessarily imply the absence of parasites. As documented for PMM treatment, relapse can be detected by BLI upon extended follow-up.[6] The absence/presence of viable parasites in the target tissues following treatment can also be supported by more sensitive techniques such as SL-RNA qPCR.[8]

**Table 1. Parasite Elimination Half-Lives ($t_{1/2}$) for the Different Treatment Groups Based on the Decline in Bioluminescent Signal Measured in the Whole Body, the Liver and the Bone Marrow**

| drug | $t_{1/2}$ in whole body (days) | $t_{1/2}$ in liver (days) | $t_{1/2}$ in bone marrow (days) |
|---|---|---|---|
| miltefosine | 2.0 ± 0.1 | 1.9 ± 0.6 | 1.5 ± 0.5 |
| paromomycin | 4.6 ± 0.4 | 4.3 ± 0.1 | 14.0 ± 4.6 |
| l-AmB | 0.4 ± 0.1 | 0.2 ± 0.1 | 0.4 ± 0.1 |

Single-dose treatment with l-AmB resulted in the fastest clearance of parasites with a reduction of relative luminescence units (RLU) values in all ROIs to the recorded levels in noninfected control mice measured only 1 day after treatment, not even when using a more sensitive BLI scale. Table 1 demonstrates $t_{1/2}$s for l-AmB of 0.2 days in the liver, 0.4 days in the bone marrow, and 0.4 days based on whole body analysis, all reflecting the swift cidal effect of this single-dose treatment (Figure 2). At 58 dpi, no parasites were detected in Giemsa-stained tissue samples and no parasite-specific BLI signal was observed on a more sensitive imaging (Figure 3), also suggesting a low probability for post-treatment relapse.

Although various bioluminescent *Leishmania* species and strains have already been used to monitor *in vitro* drug efficacy,[9,10] *in vivo* parasite fitness linked to drug resistance,[7,11] and the impact of (vaccine-induced) immune responses or interventions,[12,13] the application of BLI for *in vivo* drug potency has been scarce. Nevertheless, the kinetics of drug treatment have already been assessed in the hamster[14] and the BALB/c mouse model.[6,7,14,15] Álvarez-Velilla et al. showed that BALB/c mice were seemingly cleared of infection after 5 days of MIL treatment at 40 mg/kg/day.[15] Our previous reports used BLI to demonstrate a striking MIL dependency of a resistant *L. infantum* strain, linked to lowered NK and NKT cell responses in the liver, leading to reduced IFN-$\gamma$ production.[7,13] The differences in cidal dynamics between the reference drugs observed in this study corroborate previous findings *in vitro*, where the effect of PMM was slower than that of MIL[2]. PMM monotherapy was also found to be prone to fast relapse, originating from the bone marrow.[6] For PMM, it is well known that efficacy varies between different strains and regions,[16−21] limiting its application mainly to combination treatment with other drugs.[22−26] The comparatively slow cidal effect of AmB, documented from our previous *in vitro* work,[2] reflects the difference with the far more effective liposomal formulation of AmB. A recent study into the rate of SL-RNA decay corroborates the very fast antileishmanial effect of l-AmB. In most endemic settings, a single intravenous dose of l-AmB treatment nowadays is even the recommended first-line treatment,[27] showing high efficacy in most patients.

Although this model can discriminate between fast-, moderate-, and slower-acting drugs and can highlight


https://doi.org/10.1021/acsinfecdis.4c00109
ACS Infect. Dis. 2024, 10, 2101−2107

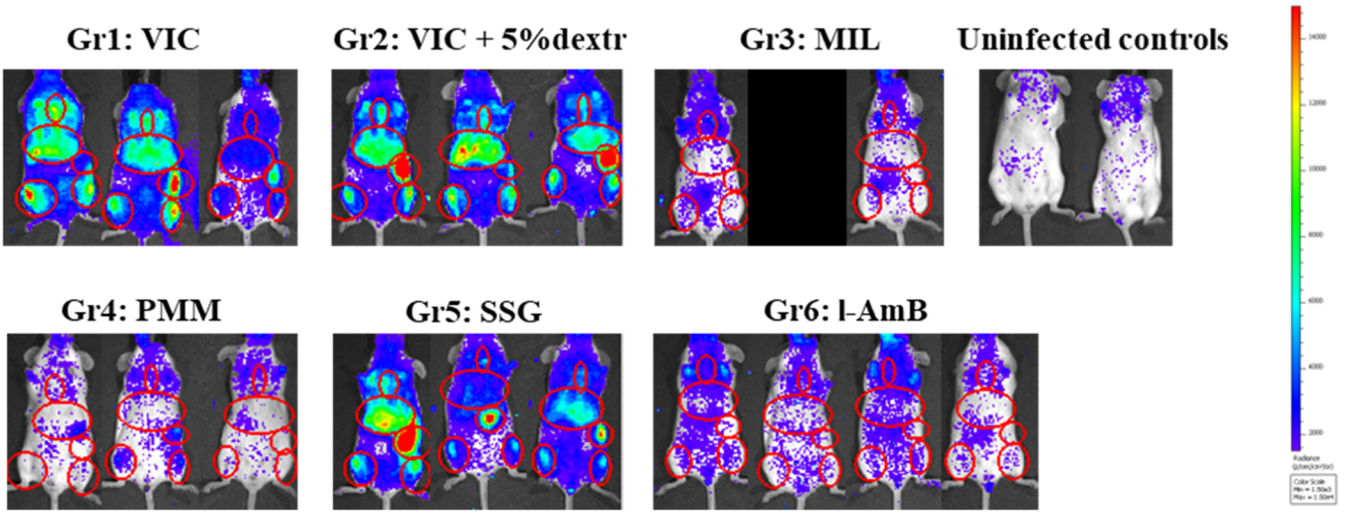


**Figure 3.** Bioluminescent images of the different treatment groups on a more sensitive scale at 58 dpi (end of study). BLI scale: $1.5e^3$-$1.5e^4$ RLU.

compounds more prone to relapse, there are some limitations to consider as well. Differences in the recorded cidal drug dynamics can be influenced by the route of administration, *i.e.*, intravenous l-AmB injection promptly targets the liver. Our study and others[15] also demonstrate the typical fluctuations in infection dynamics between different target organs. In our model, *L. infantum* causes a typical VL infection pattern with a peak in parasite burdens in liver and bone marrow at 3 weeks post-infection (wpi), and a subsequent spleen peak around 8 wpi.[7] This pattern complicates the evaluation of drug efficacy in the spleen as its colonization has not yet started in the selected treatment window. Nevertheless, the parasite burdens (and corresponding BLI signals) in the VIC groups and the SSG-treated groups remain stable during the window of treatment (Figure 3), proving that the kinetics measured in this study are in fact caused by the cidal drug activity and are not linked to the spontaneous resolution of infection. For VL, the hamster model more closely resembles human pathology with a simultaneous progressively worsening infection with involvement of liver, bone marrow, and spleen, resulting in death when left untreated. However, the application of the hamster model for BLI studies is mainly limited by the high cost of the required substrate (D-luciferin).

Collectively, this study clearly revealed differences between the different antileishmanial reference drugs and demonstrates that the applied BALB/c VL BLI model is a valuable asset for comparing cidal dynamics of NCEs administrated in monotherapy or when recommending potential combinations of slow-acting and fast-acting drugs.

## CONCLUSIONS

*In vivo* bioluminescence imaging of *Leishmania*-infected BALB/c mice, utilizing the red-shifted luciferase reporter PpyRE9, can be used in future research to assess and compare the cidal modalities of antileishmanial NCEs alone or in combination. This technique was able to accurately distinguish between fast- and slower-acting cidal reference drugs and can be used to evaluate the elimination of parasites in major target organs such as the liver, bone marrow, and the whole body as well as the kinetics thereof. It can also be used to track potential post-treatment relapse and its pattern in a longer follow-up study

## MATERIALS AND METHODS

**Ethics.** The use of laboratory animals was carried out in strict accordance with all mandatory guidelines (EU directive 2010/63/EU on the protection of animals used for scientific purpose and the Declaration of Helsinki) and was approved by the Ethical Committee of the University of Antwerp (UA-ECD-2022−85).

**Animals.** Female BALB/c mice (15−20 g) were purchased from Janvier-France and kept in quarantine for at least 5 days before starting the experiment. Food for laboratory rodents and drinking water were available *ad libitum*. Animals were randomly allocated to experimental units of 3 animals and infected on day 0 of the experiment with $10^8$ late stationary phase promastigotes.

**Artificial Infection.** A *L. infantum* isolate from a French HIV patient (CNRL, Montpellier France) was transfected earlier with the red-shifted firefly luciferase gene variant PpyRE9 that was codon-optimized for expression in *Leishmania* (GenScript) (MHOM/FR/96/LEM3323$^{PpyRE9}$).[7] This strain is resistant against antimonials and is susceptible to the antileishmanial reference drugs MIL ($IC_{50}$ = 1.0 ± 0.1 $\mu$M), PMM ($IC_{50}$ = 98.0 ± 14.3 $\mu$M), and l-AmB ($IC_{50}$ = 0.0020 ± 0.0004 $\mu$M). Promastigotes were cultured in HOMEM medium to late stationary phase in 75 mL culture flasks under 150 $\mu$g/mL hygromycin pressure. Parasites were resuspended to a concentration of $10^8$/100 $\mu$L and administered intravenously (IV) in the lateral tail vein of the mice.

**Test Substances and Formulations.** Paromomycin (PMM) and miltefosine (MIL) were formulated in water at 70 and 10 mg/mL, respectively. Sodium stibogluconate (SSG) injection solution (Albert David Ltd., Kolkata, India) was formulated in water at 51 mg/mL (equivalent of 26.14 mg/mL $Sb^v$). AmBisome (l-AmB) was formulated in 5% dextrose at a final concentration of 0.5 mg/mL to achieve a 200 $\mu$L injection volume per 20 g body weight.

**Experimental Design.** Animals were treated starting from 7 dpi, and two vehicle control groups were included because of the different vehicles involved. **Group 1** was dosed with water intraperitoneally (IP) for 5 days once daily (s.i.d.). **Group 2** was given 200 $\mu$L of 5% dextrose *via* a single intravenous (IV) injection on day 1. **Group 3** was orally (PO) treated with MIL


https://doi.org/10.1021/acsinfecdis.4c00109
ACS Infect. Dis. 2024, 10, 2101−2107

at 40 mg/kg s.i.d. for 5 days. **Group 4** was treated IP at 350 mg PMM/kg for 5 days s.i.d. **Group 5** was treated IP at 320 mg/kg SSG for 5 days s.i.d. **Group 6** was given a single IV injection of 5 mg/kg l-AmB on day 1. Because of the potential variation upon IV drug administration, an extra animal was foreseen in this group.

Parasite burdens were monitored daily for 10 days from the start of treatment and further on weekly *via* bioluminescence imaging (BLI), which was performed 3 min after IP injection of 150 mg/kg D-luciferin (Beetle Luciferin Potassium Salt, Promega) in the *IVIS Spectrum In Vivo Imaging System* (PerkinElmer) under 2−2.5% isoflurane anesthesia adopting 10 min exposure. Images were analyzed using LivingImage v4.3.1 software by drawing ROIs corresponding to the specific target organs (liver, bone marrow, whole body) to quantify the luminescent signal as relative luminescence units (RLU). Animals were followed up for 8 weeks (58 dpi) to check for post-treatment relapse. Finally, the presence of residual parasites in liver, spleen, and bone marrow was evaluated microscopically in Giemsa-stained tissue imprints upon autopsy as an indication of post-treatment relapse. By using nonlinear regression analyses on the average RLU's measured in each specific ROI, parasite elimination half-lives ($t_{1/2}$) could be determined for each target organ.

## ■ ASSOCIATED CONTENT

### Supporting Information

The Supporting Information is available free of charge at https://pubs.acs.org/doi/10.1021/acsinfecdis.4c00109.

*In vivo* bioluminescence imaging revealing differences in *Leishmania infantum* parasite killing kinetics by anti-leishmanial reference drugs (XLSX)

## ■ AUTHOR INFORMATION


### Corresponding Author

**Guy Caljon** − *Laboratory of Microbiology, Parasitology and Hygiene (LMPH), University of Antwerp, 2610 Antwerp, Belgium*; orcid.org/0000-0002-4870-3202; Phone: (32) 3/265.26.01; Email: guy.caljon@uantwerpen.be

### Authors

**Sarah Hendrickx** − *Laboratory of Microbiology, Parasitology and Hygiene (LMPH), University of Antwerp, 2610 Antwerp, Belgium*

**Pim-Bart Feijens** − *Laboratory of Microbiology, Parasitology and Hygiene (LMPH), University of Antwerp, 2610 Antwerp, Belgium*

**Fanny Escudié** − *Drugs for Neglected Diseases initiative, 1202 Geneva, Switzerland*

**Eric Chatelain** − *Drugs for Neglected Diseases initiative, 1202 Geneva, Switzerland*

**Louis Maes** − *Laboratory of Microbiology, Parasitology and Hygiene (LMPH), University of Antwerp, 2610 Antwerp, Belgium*

Complete contact information is available at: https://pubs.acs.org/10.1021/acsinfecdis.4c00109



### Funding

This work was funded by the Drugs for Neglected Diseases initiative (DNDi) and the Research Council of the University of Antwerp (TT-ZAPBOF 33049). For these activities, DNDi received funding from the Wellcome Trust, U.K.; U.K. International Development, U.K.; and for its overall mission, from Médecins Sans Frontières International. LMPH is a partner of the *Infla-Med* Centre of Excellence (www.uantwerpen.be/infla-med) and participates in COST Action CA21111 (OneHealthdrugs).

### Notes

The authors declare no competing financial interest.

## ■ ACKNOWLEDGMENTS

The authors acknowledge Margot Vleminckx for her help with the image acquisition and Prof. Dr. Laurence Lachaud who kindly provided the *L. infantum* clinical isolate. They also thank Dr. Kirsten Gillingwater for her insight at the beginning of this project, as well as colleagues at DNDi for their valuable support and scientific input during this project.


## ■ ABBREVIATIONS

BLI, bioluminescent imaging; DNDi, Drugs for Neglected Diseases initiative; dpi, days post-infection; IP, intraperitoneal; IV, intravenous; Gr, group; l-AmB, liposomal amphotericin B; MIL, miltefosine; NCE, new chemical entity; PO, per oral administration; PPM, paromomycin; RLU, relative luminescence units; ROI, region of interest; s.i.d., single-injection dose; SSG, sodium stibogluconate; $t_{1/2}$, parasite elimination half-life; TTK, time-to-kill; VL, visceral leishmaniasis; wpi, weeks post-infection

## ■ REFERENCES


(1) De Rycker, M.; Wyllie, S.; Horn, D.; Read, K. D.; Gilbert, I. H. Anti-trypanosomatid drug discovery: progress and challenges. *Nat. Rev. Microbiol.* **2023**, *21* (1), 35−50.

(2) Maes, L.; Beyers, J.; Mondelaers, A.; Van den Kerkhof, M.; Eberhardt, E.; Caljon, G.; Hendrickx, S. In vitro 'time-to-kill' assay to assess the cidal activity dynamics of current reference drugs against Leishmania donovani and *Leishmania infantum*. *J. Antimicrob. Chemother.* **2017**, *72* (2), 428−430.

(3) Van den Kerkhof, M.; Mabille, D.; Hendrickx, S.; Leprohon, P.; Mowbray, C. E.; Braillard, S.; Ouellette, M.; Maes, L.; Caljon, G.Antileishmanial aminopyrazoles: studies into mechanisms and stability of experimental drug resistance *Antimicrob. Agents Chemother.* 2020, *64*(9), e00152-20.

(4) Van den Kerkhof, M.; Mabille, D.; Chatelain, E.; Mowbray, C. E.; Braillard, S.; Hendrickx, S.; Maes, L.; Caljon, G. *In vitro* and *in vivo* pharmacodynamics of three novel antileishmanial lead series. *Int. J. Parasitol.: Drugs Drug Resist.* **2018**, *8* (1), 81−86.

(5) Mowbray, C. E.; Braillard, S.; Glossop, P. A.; Whitlock, G. A.; Jacobs, R. T.; Speake, J.; Pandi, B.; Nare, B.; Maes, L.; Yardley, V.; et al. DNDI-6148: A Novel Benzoxaborole Preclinical Candidate for the Treatment of Visceral Leishmaniasis. *J. Med. Chem.* **2021**, *64* (21), 16159−16176.

(6) Dirkx, L.; Hendrickx, S.; Merlot, M.; Bulté, D.; Starick, M.; Elst, J.; Bafica, A.; Ebo, D. G.; Maes, L.; Van Weyenbergh, J.; Caljon, G. Long-term hematopoietic stem cells as a parasite niche during treatment failure in visceral leishmaniasis. *Commun. Biol.* **2022**, *5* (1), No. 626, DOI: 10.1038/s42003-022-03591-7.

(7) Eberhardt, E.; Bulte, D.; Van Bockstal, L.; Van den Kerkhof, M.; Cos, P.; Delputte, P.; Hendrickx, S.; Maes, L.; Caljon, G. Miltefosine enhances the fitness of a non-virulent drug-resistant *Leishmania infantum* strain. *J. Antimicrob. Chemother.* **2018**, *74*, 395−406, DOI: 10.1093/jac/dky450.

(8) Hendrickx, R. M. R.; Tadesse, D.; Teferi, T.et al. Spliced-leader RNA as a dynamic marker for monitoring viable Leishmania parasites during and after treatment *J. Infect. Dis.* 2024, in press.

(9) Lang, T.; Goyard, S.; Lebastard, M.; Milon, G. Bioluminescent Leishmania expressing luciferase for rapid and high throughput screening of drugs acting on amastigote-harbouring macrophages and

for quantitative real-time monitoring of parasitism features in living mice. *Cell. Microbiol.* **2005**, *7* (3), 383−392.
(10) Paloque, L.; Vidal, N.; Casanova, M.; Dumètre, A.; Verhaeghe, P.; Parzy, D.; Azas, N. A new, rapid and sensitive bioluminescence assay for drug screening on Leishmania. *J. Microbiol. Methods* **2013**, *95* (3), 320−323.
(11) Van Bockstal, L.; Bulté, D.; Hendrickx, S.; Sadlova, J.; Volf, P.; Maes, L.; Caljon, G. Impact of clinically acquired miltefosine resistance by *Leishmania infantum* on mouse and sand fly infection. *Int. J. Parasitol.: Drugs Drug Resist.* **2020**, *13*, 16−21.
(12) Ong, H. B.; Clare, S.; Roberts, A. J.; Wilson, M. E.; Wright, G. J. Establishment, optimization and quantitation of a bioluminescent murine infection model of visceral leishmaniasis for systematic vaccine screening. *Sci. Rep.* **2020**, *10* (1), No. 4689.
(13) Bulté, D.; Van Bockstal, L.; Dirkx, L.; Van den Kerkhof, M.; De Trez, C.; Timmermans, J. P.; Hendrickx, S.; Maes, L.; Caljon, G. Miltefosine enhances infectivity of a miltefosine-resistant *Leishmania infantum* strain by attenuating its innate immune recognition. *PLoS Neglected Trop. Dis.* **2021**, *15* (7), No. e0009622.
(14) Reimão, J. Q.; Oliveira, J. C.; Trinconi, C. T.; Cotrim, P. C.; Coelho, A. C.; Uliana, S. R. Generation of luciferase-expressing *Leishmania infantum* chagasi and assessment of miltefosine efficacy in infected hamsters through bioimaging. *PLoS Neglected Trop. Dis.* **2015**, *9* (2), No. e0003556.
(15) Álvarez-Velilla, R.; Gutiérrez-Corbo, M. d. C.; Punzón, C.; Pérez-Pertejo, M. Y.; Balaña-Fouce, R.; Fresno, M.; Reguera, R. M. A chronic bioluminescent model of experimental visceral leishmaniasis for accelerating drug discovery. *PLoS Neglected Trop. Dis.* **2019**, *13* (2), No. e0007133.
(16) Hailu, A.; Musa, A.; Wasunna, M.; Balasegaram, M.; Yifru, S.; Mengistu, G.; Hurissa, Z.; Hailu, W.; Weldegebreal, T.; Tesfaye, S.; et al. Geographical variation in the response of visceral leishmaniasis to paromomycin in East Africa: a multicentre, open-label, randomized trial. *PLoS Neglected Trop. Dis.* **2010**, *4* (10), No. e709.
(17) Llanos-Cuentas, A.; Echevarria, J.; Seas, C.; Chang, E.; Cruz, M.; Alvarez, E.; Rosales, E.; Campos, P.; Bryceson, A. Parenteral aminosidine is not effective for Peruvian mucocutaneous leishmaniasis. *Am. J. Trop. Med. Hyg.* **2007**, *76* (6), 1128−1131.
(18) Mishra, J.; Madhubala, R.; Singh, S. Visceral and post-Kala-Azar dermal leishmaniasis isolates show significant difference in their in vitro drug susceptibility pattern. *Parasitol. Res.* **2013**, *112* (3), 1001−1009.
(19) Musa, A. M.; Younis, B.; Fadlalla, A.; Royce, C.; Balasegaram, M.; Wasunna, M.; Hailu, A.; Edwards, T.; Omollo, R.; Mudawi, M.; et al. Paromomycin for the treatment of visceral leishmaniasis in Sudan: a randomized, open-label, dose-finding study. *PLoS Neglected Trop. Dis.* **2010**, *4* (10), No. e855.
(20) Neva, F. A.; Ponce, C.; Ponce, E.; Kreutzer, R.; Modabber, F.; Olliaro, P. Non-ulcerative cutaneous leishmaniasis in Honduras fails to respond to topical paromomycin. *Trans. R. Soc. Trop. Med. Hyg.* **1997**, *91* (4), 473−475.
(21) Sundar, S.; Chakravarty, J. Paromomycin in the treatment of leishmaniasis. *Expert Opin. Invest. Drugs* **2008**, *17* (5), 787−794.
(22) Musa, A.; Khalil, E.; Hailu, A.; Olobo, J.; Balasegaram, M.; Omollo, R.; Edwards, T.; Rashid, J.; Mbui, J.; Musa, B.; et al. Sodium stibogluconate (SSG) & paromomycin combination compared to SSG for visceral leishmaniasis in East Africa: a randomised controlled trial. *PLoS Neglected Trop. Dis.* **2012**, *6* (6), No. e1674, DOI: 10.1371/journal.pntd.0001674.
(23) Rijal, S.; Sundar, S.; Mondal, D.; Das, P.; Alvar, J.; Boelaert, M. Eliminating visceral leishmaniasis in South Asia: the road ahead. *BMJ* **2019**, *364*, No. k5224, DOI: 10.1136/bmj.k5224.
(24) Seaman, J.; Pryce, D.; Sondorp, H. E.; Moody, A.; Bryceson, A. D.; Davidson, R. N. Epidemic visceral leishmaniasis in Sudan: a randomized trial of aminosidine plus sodium stibogluconate versus sodium stibogluconate alone. *J. Infect. Dis.* **1993**, *168* (3), 715−720.
(25) Shazad, B.; Abbaszadeh, B.; Khamesipour, A. Comparison of topical paromomycin sulfate (twice/day) with intralesional meglumine antimoniate for the treatment of cutaneous leishmaniasis caused by L. major. *Eur. J. Dermatol.* **2005**, *15* (2), 85−87.
(26) Sundar, S.; Jha, T. K.; Thakur, C. P.; Sinha, P. K.; Bhattacharya, S. K. Injectable paromomycin for Visceral leishmaniasis in India. *N. Engl. J. Med.* **2007**, *356* (25), 2571−2581.
(27) Frézard, F.; Aguiar, M. M. G.; Ferreira, L. A. M.; Ramos, G. S.; Santos, T. T.; Borges, G. S. M.; Vallejos, V. M. R.; De Morais, H. L. O. Liposomal Amphotericin B for Treatment of Leishmaniasis: From the Identification of Critical Physicochemical Attributes to the Design of Effective Topical and Oral Formulations. *Pharmaceutics* **2023**, *15* (1), No. 99, DOI: 10.3390/pharmaceutics15010099.